

Chemistry of Cobalt Acetate. 7. Electrochemical Oxidation of μ_3 -Oxo-Centered Cobalt(III) Acetate Trimers

James K. Beattie,* Corina U. Beck, Peter A. Lay, and Anthony F. Masters

Centre for Heavy Metals Research, School of Chemistry, University of Sydney, NSW 2006, Australia

Received May 23, 2003

Electrochemical and spectroelectrochemical properties of five cobalt(III) acetate complexes $[\text{Co}^{\text{III}}_3(\mu_3\text{-O})(\text{CH}_3\text{-CO}_2)_5(\text{OR})(\text{py})_3][\text{PF}_6]$ are described, where py = pyridine and R = OCCH_3 (A), H (B), CH_3 (C), $\text{CH}_2\text{CH}=\text{CH}_2$ (D), and $\text{CH}_2\text{C}_6\text{H}_5$ (E). Each is reduced irreversibly as observed by cyclic voltammetry at room temperature and at -40°C in acetonitrile at scan rates up to 20 V s^{-1} , but oxidized reversibly to a mixed-valence $\text{Co(III)}_2\text{Co(IV)}$ species at $\sim 1.23\text{ V}$ vs the ferrocenium/ferrocene couple. Controlled potential coulometry confirmed a one-electron-oxidation process. Spectroelectrochemical oxidation of A at 5°C showed isosbestic points in the electronic absorption spectrum that showed the oxidized complex to be stable in solution for at least 1 h.

Introduction

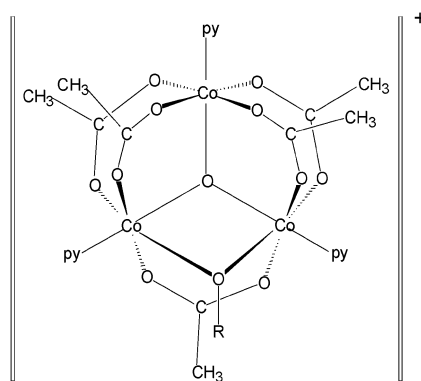
The cobalt-catalyzed autoxidation of *p*-xylene to terephthalic acid in acetic acid is of enormous industrial importance with large quantities of terephthalic acid being produced for the manufacture of poly(ethylene terephthalate) (PET).¹ Despite this, the identities of the cobalt complexes involved in the catalysis are still uncertain.²

The nature of “cobaltic acetate” is complex, with a wide variety of complexes and structures isolated from the system under different conditions.³ Of interest for the present work are the oxo-centered trimers, a common structural motif for carboxylate transition metal complexes.⁴

Uemura, Spencer, and Wilkinson⁵ added portions of pyridine or β -picoline to the product obtained by ozonization of cobaltous acetate tetrahydrate in acetic acid and showed that the stoichiometry was the same as those of oxo-centered trimers of other transition metals. They thus formulated the complexes as $[\text{Co}_3\text{O}(\text{CH}_3\text{CO}_2)_6(\text{L})_3][\text{ClO}_4]$ (L = pyridine or β -picoline). Based on their spectroscopic studies, however, they concluded that the structure of the Co complex differed

from that of the other known structures and that it contained both bridging and chelating acetate groups.

In 1985 Sumner and Steinmetz⁶ found that treatment of an acetic acid solution of cobaltous acetate, pyridine, and ammonium hexafluorophosphate with peracetic acid resulted in the immediate formation of a solid mixture. Single-crystal X-ray diffraction was used to characterize $[\text{Co}^{\text{III}}_3(\mu_3\text{-O})(\text{CH}_3\text{CO}_2)_5(\text{OH})(\text{py})_3]^+$ as its $[\text{Co}(\text{py})(\text{Br})_3]^-$ salt.



Sumner and Steinmetz also synthesized a family of oxo-centered cobalt(III) cluster complexes bridged by alkoxide ligands. These were prepared by the treatment of $[\text{Co}^{\text{III}}_3(\mu_3\text{-O})(\text{CH}_3\text{CO}_2)_6(\text{py})_3][\text{PF}_6]$ with alcohols in refluxing acetonitrile,⁷ and they examined the catalytic activity of two

* Corresponding author. E-mail: beattiej@chem.usyd.edu.au.

- (1) Partenheimer, W.; Gipe, R. K. In *Catalytic Selective Oxidation*; Oyama, S. T., Hightower, J. W., Eds.; American Chemical Society: Washington, DC, 1993; Vol. 523, p 81.
- (2) Jiao, X.-D.; Espenson, J. H. *Inorg. Chem.* **2000**, *39*, 1549.
- (3) Beattie, J. K.; Hambley, T. W.; Klepetko, J. A.; Masters, A. F.; Turner, P. *Polyhedron* **1998**, *17*, 1343.
- (4) Cannon, R. D.; White, R. P. *Prog. Inorg. Chem.* **1988**, *36*, 195.
- (5) Uemura, S.; Spencer, A.; Wilkinson, G. *J. Chem. Soc., Dalton Trans.* **1973**, 2565.

- (6) Sumner, C. E. J.; Steinmetz, G. R. *J. Am. Chem. Soc.* **1985**, *107*, 6124.
- (7) Sumner, C. E. J.; Steinmetz, G. R. *Inorg. Chem.* **1989**, *28*, 4290.

oxo-centered trimeric complexes, $[\text{Co}^{\text{III}}_3(\mu_3\text{-O})(\text{CH}_3\text{CO}_2)_5\text{-OR}(\text{py})_3]^+$, where $\text{R} = \text{OCCH}_3$ or H .⁶ They showed that by warming a mixture of these complexes with toluene and LiBr in acetic acid in the absence of oxygen, benzyl bromide was formed in large quantities (93% of theoretical). When carried out under aerobic conditions, the reaction became autocatalytic and toluene was preferentially converted to benzoic acid. The same catalytic system was also employed for the oxidation of xylene, where it was observed to produce 65 equivalents (equiv) of product $\text{h}^{-1} \text{mol}^{-1}$ of cobalt in the presence of oxygen. The use of a CoBr_2 catalyst, on the other hand, resulted in only 23 equiv of product $\text{h}^{-1} \text{mol}^{-1}$ of cobalt. These results suggested that the trimeric complexes could be successfully used as catalyst precursors for the autoxidation of aromatic hydrocarbons.

Further autoxidation studies revealed that the oxo-centered cobalt trimers could be isolated from reactions to which they were not initially introduced. Sumner and Steinmetz found that both $[\text{Co}^{\text{III}}_3(\mu_3\text{-O})(\text{CH}_3\text{CO}_2)_5(\text{OH})(\text{py})_3]^+$ and $[\text{Co}^{\text{III}}_3(\mu_3\text{-O})(\text{CH}_3\text{CO}_2)_6(\text{py})_3]^+$ formed in relatively large quantities (32% yield) when air was bubbled through a warm acetic acid solution containing cobalt acetate, pyridine, NH_4PF_6 , and a small amount of HBr to oxidize *p*-xylene.⁶ They suggested that the in situ formation of such trimers might be responsible for the dramatic rate increase observed when pyridine is added to the cobalt bromide catalyzed autoxidation of *p*-xylene.

The current work examines the electrochemical behavior of a number of these complexes, $[\text{Co}^{\text{III}}_3(\mu_3\text{-O})(\text{CH}_3\text{CO}_2)_5\text{-OR}(\text{py})_3]^+$ ($\text{R} = \text{OCCH}_3$, H , CH_3 , $\text{CH}_2\text{CH}=\text{CH}_2$, and $\text{CH}_2\text{-Ph}$). The aim was to investigate the potentials at which these species are oxidized and reduced and also to determine what effect the unique ligand has on the redox behavior of the complexes. In previous work, the redox chemistry of the β -picoline complex obtained by Uemura and co-workers, $[\text{Co}^{\text{III}}_3\text{O}(\text{CH}_3\text{CO}_2)_6(\beta\text{-pic})_3]\text{ClO}_4$, had been examined in acetone/ NaClO_4 via polarography.⁵ An irreversible, one-electron-reduction wave was reported at $E_{1/2} = +0.13 \text{ V}$ vs SCE, but no oxidation processes were observed. Attempts made to isolate this reduced species following coulometric reduction were unsuccessful. The cluster, $[\text{Co}^{\text{III}}_3\text{O}(\text{CO}_2\text{-CH}_3)_6(\text{CH}_3\text{CO}_2\text{H})_3]^+$, was reported to be reduced in two separate steps via polarography.⁸ The first reduction was ascribed to the reduction of one $\text{Co}(\text{III})$ to $\text{Co}(\text{II})$. The second was suggested to result from the reduction of $\text{Co}(\text{II})$ to $\text{Co}(0)$. The potentials at which these reductions occurred were not reported.

Experimental Section

The complexes were prepared by the methods of Sumner and Steinmetz⁶ and characterized by ^1H NMR spectroscopy as described elsewhere.⁹

Tetrabutylammonium tetrafluoroborate (TBATFB) (Aldrich, electrochemical grade) was recrystallized three times from ethyl

acetate/diethyl ether and dried under vacuum. Tetrabutylammonium hexafluorophosphate (TBAH) (Fluka, electrochemical grade) was recrystallized from ethanol/water and dried for 10 h at 70°C under vacuum. Tetrabutylammonium perchlorate (TBAP) (Fluka, electrochemical grade) was recrystallized from diethyl ether/acetone and dried over P_2O_5 under a vacuum at room temperature.

Electrochemical measurements were performed using a BAS 100B electrochemical analyzer equipped with a BAS C2 cell stand. Electrochemical data were collected and analyzed using BAS 100W version 2.0 software. Cyclic voltammetry (CV) was conducted using a three-electrode system with 100% *iR* compensation being applied. The experiments were performed in a 10-mL sample cell having a lid designed for a three-electrode configuration. The working electrode employed was either a 3-mm-diameter glassy carbon (GC) inlaid disk electrode or a 1.2-mm-diameter Pt disk electrode. This electrode was polished three times between each run with diamond pastes of decreasing particle size (1, 0.25, and $0.10 \mu\text{m}$) and glycerin on a Mecaprex polishing cloth. After polishing, the electrode was allowed to equilibrate for ca. 5 min in the electrolytic solution being examined. All experiments at room temperature ($22 \pm 1^\circ\text{C}$) involved the use of a saturated $\text{Ag}/\text{AgCl}/\text{NaCl}$ (3 M) reference electrode and Pt wire counter electrode (0.5 mm diameter, 5 cm length). Experiments were also performed in a nonisothermal cell at ca. $-40 \pm 5^\circ\text{C}$. In these cases, the solutions were cooled to $-40 \pm 5^\circ\text{C}$ in a $\text{CH}_3\text{CN}/\text{CO}_2(\text{s})$ bath. The cell design and electrodes employed were the same as described for experiments at room temperature, with the exception that a Ag/AgNO_3 (3 M in CH_3CN) reference electrode was employed to avoid freezing.

All electrochemical samples were purged and kept under a continuous flow of ultrahigh purity Ar (BOC). An argon purification assembly was employed which consisted of an indicating moisture trap (5-Å molecular sieves with Dryerite, Activon, RDMT400D), a high capacity coiled O_2 trap (oxy-trap, Alltech, 4003), and an indicating O_2 trap (indicating oxy-trap, Alltech, 4004). The flow of the purified Ar was then regulated using a gas flowmeter (Cole Parmer, brass, standard valve, H 03297-00). The purified Ar was passed through a bubbler containing only the relevant solvent (CH_3CN or CH_2Cl_2) before entering the electrochemical cell. Solvent saturated Ar was then bubbled through the experimental solution for ca. 30 min prior to the first CV experiment and for at least 5 min between each CV run. All studies were performed inside a Faraday cage in order to reduce electromagnetic interference.

The Co acetate trimers, $[\text{Co}^{\text{III}}_3(\mu_3\text{-O})(\text{CH}_3\text{CO}_2)_5(\text{OR})(\text{py})_3][\text{PF}_6]$ ($\text{R} = \text{OCCH}_3$, H , CH_3 , CH_2CHCH_2 , CH_2Ph), were each examined at room temperature in $\text{CH}_3\text{CN}/\text{TBAH}$ (0.1 M) at a concentration of 10^{-3} M . Solutions of these trimers (again 10^{-3} M) were also examined at $-40 \pm 5^\circ\text{C}$ as described above. Both GC and Pt working electrodes were used with similar results. Experiments were also performed (at 22 and -40°C) in which an excess of pyridine (0.4 mL, $5 \times 10^{-3} \text{ M}$) was added to the electrochemical solution. In all cases, the results were referenced against the $[\text{Fe}(\eta^5\text{-C}_5\text{H}_5)_2]^{+0}$ couple measured with the same cell configuration.

Bulk electrolysis was performed using an EG&G Princeton Applied Research Model 273A potentiostat/galvanostat. The solution resistance was compensated with the use of a 20 MHz Hitachi Model V212 oscilloscope. Data were collected using Headstart Software. Controlled potential electrolysis was performed on each of the Co trimers. Solutions (20 mL, $5 \times 10^{-4} \text{ M}$ in $\text{CH}_3\text{CN}/\text{TBAH}$ (0.1 M)) were introduced into a glass electrochemical cell composed of two compartments separated by a sintered glass frit of porosity 3. One compartment contained both the working electrode, which in each case was a Pt mesh basket, and a $\text{Ag}/\text{AgCl}/\text{NaCl}$ (3 M) reference electrode. The second compartment contained a Pt mesh

(8) Ziolkowski, J. J.; Pruchnik, F.; Szymanska-Buzar, T. *Inorg. Chim. Acta* **1973**, *7*, 473.

(9) Beattie, J. K.; Klepetko, J. A.; Masters, A. F.; Turner, P. *Polyhedron* **2003**, *22*, 947.

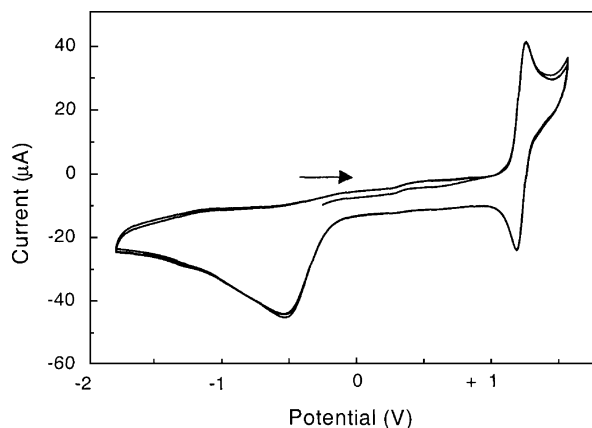


Figure 1. Cyclic voltammogram of 10^{-3} M $[\text{Co}^{\text{III}}_3(\mu_3\text{-O})(\text{CH}_3\text{CO}_2)_6(\text{py})_3]\cdot[\text{PF}_6]_3$, **A**, in $\text{CH}_3\text{CN}/\text{TBAH}$ (0.1 M) at GC electrode at 22 ± 1 °C; scan rate = 0.100 V s^{-1} ; 100% *iR* compensation. The potential sweep was commenced at -0.250 V .

counter electrode. The solutions were stirred continually and were maintained at a temperature of 5 ± 2 °C by immersing the cell in an ice/water slurry. Each solution was purged with Ar gas for ca. 30 min prior to electrolysis. Controlled potential coulometry was performed on these solutions at potentials ca. 0.100 V more positive than the $E_{1/2}$ values of the trimers ($+1.35 \text{ V}$ vs $[\text{Fe}(\eta^5\text{-C}_5\text{H}_5)_2]^{+/0}$) until the current was approximately 1% of its original value.

Electronic spectra of solutions were obtained using a Hewlett-Packard 8452A diode array spectrophotometer equipped with a Peltier variable temperature device. The electronic spectra of the Co trimers were examined over the wavelength range 280–800 nm in a 1 cm path length quartz cell. The concentration of each solution was 5×10^{-4} M in CH_3CN .

The spectral changes in the electronic spectrum of $[\text{Co}^{\text{III}}_3(\mu_3\text{-O})(\text{CH}_3\text{CO}_2)_6(\text{py})_3][\text{PF}_6]_3$ during bulk electrolysis were examined in a optically transparent thin layer electrode (OTTLE) cell of 1 mm path length. A solution of this complex (1.7 mL, 5×10^{-3} M in $\text{CH}_3\text{CN}/\text{TBAH}$ (0.1 M)) was introduced into the OTTLE cell and oxidized at $+1.35 \text{ V}$ vs $[\text{Fe}(\eta^5\text{-C}_5\text{H}_5)_2]^{+/0}$. A three-electrode system was again employed in which the working electrode was a Pt mesh OTTLE. A Pt mesh basket counter electrode and a Ag/AgCl/NaCl (3 M) reference electrode were also used. The temperature of the system was kept at a constant 5 ± 2 °C, and the spectral changes in the region 380–700 nm were monitored every 5 min over the course of 1 h. The *iR* drop due to the solution resistance was uncompensated.

Results

Cyclic Voltammetry (CV). The CV behavior of all five Co trimers was similar. Each complex exhibited a broad, irreversible, reductive process and a reversible oxidative process within the potential range examined. A typical full-scan CV is shown in Figure 1.

CV Reduction of Trimers. Each of the complexes displayed irreversible reduction waves consisting of at least three separate processes that extended over $\sim 1 \text{ V}$. The first of these was readily discerned at all scan rates from 0.100 to 20.480 V s^{-1} . The others were ill-defined shoulders that were observed at more negative potentials than the first and broadened to such an extent that they were difficult to distinguish at scan rates $> 5 \text{ V s}^{-1}$. Measurements were made at ca. -40 °C in order to determine whether the reductive

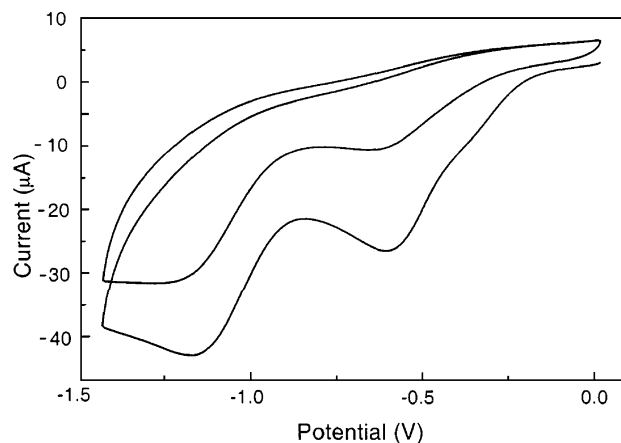


Figure 2. Cyclic voltammogram of $[\text{Co}^{\text{III}}_3(\mu_3\text{-O})(\text{CH}_3\text{CO}_2)_6(\text{py})_3][\text{PF}_6]_3$, **A** (10^{-3} M), with pyridine (0.4 mL, 5 mM) in $\text{CH}_3\text{CN}/\text{TBAH}$ (0.1 M) at GC electrode at 22 ± 1 °C; scan rate = 0.300 V s^{-1} ; 100% *iR* compensation. Potential sweep was commenced at $+0.020 \text{ V}$ and reversed at -1.435 V .

processes could be made reversible, but they remained irreversible at scan rates up to 20 V s^{-1} at -40 °C regardless of the potentials at which the CV scan was commenced or reversed.

The redox behavior of each of the trimers was examined in the presence of excess pyridine (0.4 mL, 5 mM) to determine whether this would lead to reversible reduction processes, as had been observed for analogous Fe(III) complexes.¹⁰ Two well-defined reduction waves were observed: the first, which consisted of two processes, occurred at potentials (ca. -0.6 V) similar to those in the absence of pyridine; the second occurred (ca. -1.2 V) at more negative potentials than previously observed (Figure 2). These reductions were irreversible over all scan rates applied (0.100 – 20.480 V s^{-1}). When the potential was reversed at -0.865 V , the first two reduction processes remained irreversible. Pyridine in $\text{CH}_3\text{CN}/\text{TBAH}$ was not reduced over the potential range examined ($+0.180$ to -1.835 V).

CV Oxidation of Trimers. At scan rates $> 0.300 \text{ V s}^{-1}$ for **A**, **C**, **D**, and **E** and $> 1.101 \text{ V s}^{-1}$ for **B**, the chemically reversible oxidative processes observed in the cyclic voltammograms of the Co trimers were nearly identical (Figure 3).

At slower scan rates ($< 0.300 \text{ V s}^{-1}$ for **A**, **C**, **D**, and **E**; $< 1.101 \text{ V s}^{-1}$ for **B**) a shoulder on the oxidation wave was also observed, but only on the first scan for each of the complexes (Figure 4). This is indicative of a slow preequilibrium of a minor species with the major trimeric complex, which is then consumed by a cross-reaction with the major oxidized species and does not appear on subsequent scans, or when the scan rate is too rapid for the equilibrium to be maintained as the minor species is oxidized.

The CV of **B**, the hydroxo-bridged complex, at slow scan rates ($< 1.101 \text{ V s}^{-1}$) differed from those of the other complexes by the presence of two chemically reversible couples (Figure 5). The potentials at which the additional process occurred ($E_{\text{pa}} = +1.390 \text{ V}$ and $E_{\text{pc}} = +1.333 \text{ V}$)

(10) Bond, A. M.; Clark, R. J. H.; Humphrey, D. G.; Panayiotopoulos, P.; Skelton, B. W.; White, A. H. *J. Chem. Soc., Dalton Trans.* **1998**, 1845.

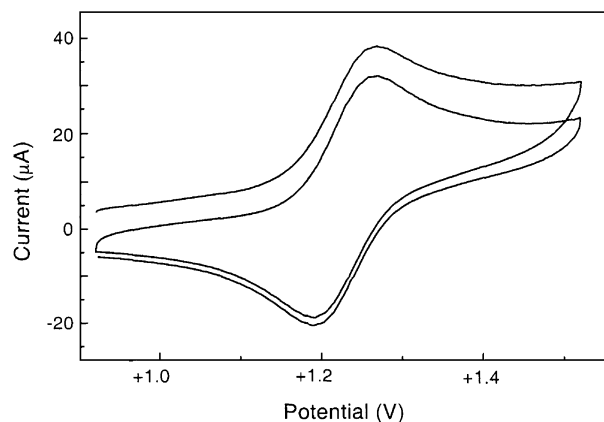


Figure 3. CV of $[\text{Co}^{\text{III}}_3(\mu_3\text{-O})(\text{CH}_3\text{CO}_2)_6(\text{py})_3][\text{PF}_6]$, **A** (10^{-3} M), in $\text{CH}_3\text{CN}/\text{TBAH}$ (0.1 M) at GC electrode at 22 ± 1 °C; scan rate = 1.204 V s^{-1} ; 100% iR compensation. Potential sweep commenced at +0.920 V and reversed at +1.520 V.

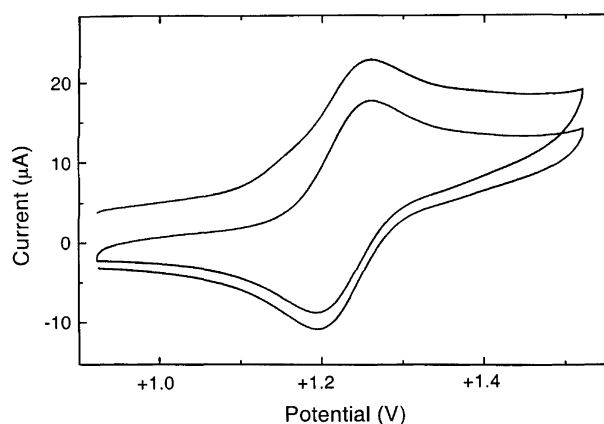


Figure 4. Cyclic voltammogram of $[\text{Co}^{\text{III}}_3(\mu_3\text{-O})(\text{CH}_3\text{CO}_2)_6(\text{py})_3][\text{PF}_6]$, **A** (10^{-3} M), in $\text{CH}_3\text{CN}/\text{TBAH}$ (0.1 M) at GC electrode at 22 ± 1 °C; scan rate = 0.100 V s^{-1} ; 100% iR compensation. Potential sweep commenced at +0.920 V and reversed at +1.520 V.

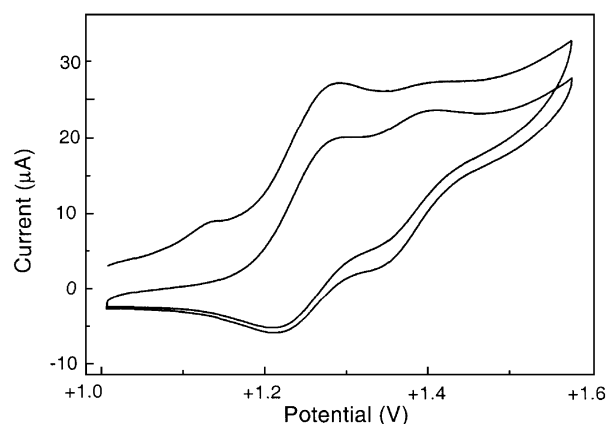


Figure 5. CV of $[\text{Co}^{\text{III}}_3(\mu_3\text{-O})(\text{CH}_3\text{CO}_2)_5(\text{OH})(\text{py})_3][\text{PF}_6]$, **B** (10^{-3} M), in $\text{CH}_3\text{CN}/\text{TBAH}$ (0.1 M) at GC electrode at 22 ± 1 °C; scan rate = 0.100 V s^{-1} ; 100% iR compensation. Potential sweep commenced at +1.005 V and reversed at +1.575 V.

were unchanged as the scan rate was increased and also remained constant on subsequent sweep cycles. Their peak-to-peak separation was 0.057 V at all scan rates. As the scan rate was raised, both processes decreased in intensity until, at scan rates $>1.101 \text{ V s}^{-1}$, neither process was visible. Furthermore, at 5 °C even at slow scan rates, the CVs were identical to the fast scan rate CVs obtained at room

Table 1. Electrochemical Data for Chemically Reversible Oxidations of 10^{-3} M $[\text{Co}^{\text{III}}_3(\mu_3\text{-O})(\text{CH}_3\text{CO}_2)_5(\text{OR})(\text{py})_3][\text{PF}_6]$ in $\text{CH}_3\text{CN}/\text{TBAH}$ (0.1 M) at GC Electrode at 22 ± 1 °C with 100% iR Compensation^a

R	I_{pa}/I_{pc}		ΔE_p (V)		$E_{1/2}$ (V)
	0.100 V s^{-1}	1.204 V s^{-1}	0.100 V s^{-1}	1.204 V s^{-1}	
OCCH ₃ (A)	1.15	1.24	0.056	0.064	+1.231
H (B)	3.09	1.29	0.084	0.150	+1.257
CH ₃ (C)	1.24	1.18	0.065	0.089	+1.248
CH ₂ CHCH ₂ (D)	1.29	1.33	0.061	0.064	+1.224
CH ₂ C ₆ H ₅ (E)	1.35	1.28	0.062	0.074	+1.215

^a Potentials vs $[\text{Fe}(\eta^5\text{-C}_5\text{H}_5)_2]^+/\text{0}$.

temperature and only a single reversible oxidation was observed. This suggests a second oxidation reaction of a minor species that occurs only after a slow transformation of the first oxidized product. It is perhaps significant that this feature is seen only for the unique hydroxo-bridged species that might undergo deprotonation on oxidation and not with the other carboxylate- or alkoxy-bridged trimers.

Table 1 summarizes the data for the reversible oxidation processes. The ratio of the anodic to cathodic currents is in the range 1.1–1.3 for each of the complexes at both slow and fast scans, except for **B** at slow scans. The peak-to-peak separations range from 61 to 89 mV, except for complex **B** at fast scans. The half-wave potentials are nearly constant, and independent of scan rate, ranging from 1.21 to 1.26 V.

Coulometry. Controlled potential coulometry was performed at potentials close to those at which the reversible oxidative process was observed for each trimer. The solutions of **B**, **C**, **D**, and **E** were initially yellowish brown and became more reddish brown as the oxidation progressed, whereas that of **A** was initially reddish brown and became wine red. The charge transferred to each trimer during the course of electrolysis corresponded to approximately one electron per trimer (1.05, 1.14, 1.20, 0.96, and 1.17 for **A**, **B**, **C**, **D**, and **E**, respectively).

Spectroelectrochemistry. In situ electrochemical oxidation with an OTTLE cell was undertaken to examine the stability of the oxidized complexes over a longer time period. Only the symmetric trimer, complex **A**, was examined spectroelectrochemically.

The electronic spectrum of **A** is unique among the five trimers in that it exhibits a well-defined absorption at ca. 484 nm ($\epsilon_{\text{max}} \approx 1920 \text{ M}^{-1} \text{ cm}^{-1}$) and a weak shoulder at ca. 600 nm ($\epsilon_{\text{max}} \approx 640 \text{ M}^{-1} \text{ cm}^{-1}$). The other complexes display only broad, weak shoulders on the edge of the charge-transfer band.

Spectral changes between 380 and 700 nm were recorded every 5 min for 1 h during the oxidation of a solution of **A** in a 1 mm path length OTTLE cell (Figure 6). As the oxidation progressed, the intensity of the dominant absorption at ca. 484 nm decreased until only a shoulder remained. The intensity of the slight shoulder absorption at ca. 600 nm remained relatively unchanged. The isosbestic point at 444 nm indicates that only two species were present in the solution at any one time and demonstrates that the oxidized species is remarkably stable at 5 °C over 1 h without decomposition.

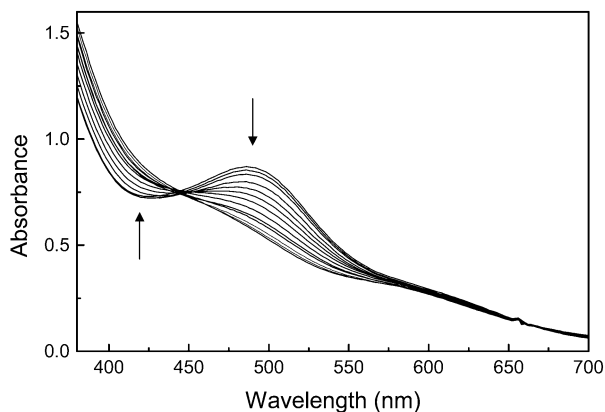


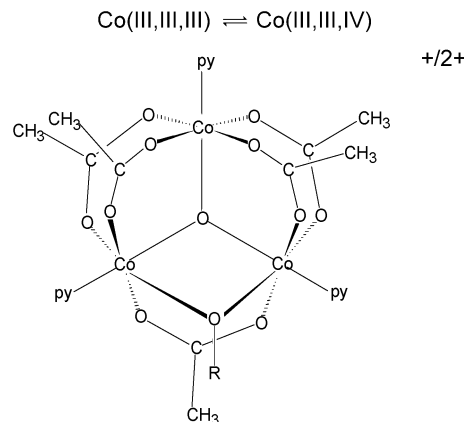
Figure 6. Electronic absorption spectral changes at 5 min intervals during oxidation at +1.35 V vs 5×10^{-3} M $[\text{Fe}(\eta^5\text{-C}_5\text{H}_5)_2]^{+/0}$. $[\text{Co}^{\text{III}}_3(\mu_3\text{-O})(\text{CH}_3\text{-CO}_2)_6(\text{py})_3][\text{PF}_6]$ in $\text{CH}_3\text{CN}/0.1$ M TBATFB at 5 °C.

Discussion

The reduction of the cobalt(III) oxo-centered trimers is irreversible, at least on the millisecond time scale of the fastest cyclic voltammetry sweep, even at -40 °C in acetonitrile. In the presence of excess pyridine, subsequent redox processes at more negative potentials occur, but again are irreversible. This contrasts with the electrochemical behavior of similar Fe(III) trimers where the addition of pyridine turned an irreversible reduction into a reversible one.¹⁰ Irreversible reductions of Co(III) to Co(II) are common, however, due to the lability of Co(II).

If this irreversibility extends to solutions of the complexes in acetic acid at higher temperatures, it casts some doubt on the proposed role of these trimers as catalysts in cobalt acetate catalyzed autoxidation reactions. They may still act as initiators to generate radicals, but their reformation to participate in another catalytic cycle would require a more complex mechanism than simple reoxidation.

Remarkably, the trimeric Co(III) complexes are reversibly oxidized in a one-electron step to a mixed-valence, formally Co(III,III,IV) species. Electron paramagnetic resonance spectra to be described elsewhere indicate that the three cobalt atoms are equivalent and that the charge on the mixed-valence species is delocalized. Cobalt(IV) complexes are rare. A recently reported example involves a tetraoxocubane complex, $[\text{Co}_4\text{O}_4(\text{O}_2\text{CR})_2(\text{bpy})_4]^{3+}$, which is also described



as a delocalized species.¹¹ This complex possesses a cubane $[\text{Co}_4(\mu_3\text{-O})_4]^{5+}$ core which bears some similarity to the trimers examined in this work in that the Co atoms are bridged by oxo (O^{2-}) and acetato (CH_3CO_2^-) ligands. Among the μ_3 -oxo complexes of the other first-row transition metals, only vanadium is known in the IV oxidation state, in what was termed a “deviant” structure, with two $\text{V}=\text{O}$ groups and an asymmetric μ_3 -oxygen atom in $[\text{V}_3\text{O}_3(\text{PhCO}_2)_6(\text{THF})]$.¹²

The reversibility of the oxidation is explicable when the electronic structure of the trimers is considered. According to a qualitative MO description, the HOMO is a π -antibonding orbital centered on the μ_3 -oxygen atom. In this case removal of one electron would have little effect on the structure, accounting for both the reversibility of the oxidation process and the similarity of the redox potentials among the five complexes with different bridging ligands.

Although the oxidation potentials for these Co(IV) species are high, the existence of this oxidation state in reversible, electron-transfer reactions with the Co(III) analogues introduces new possibilities to consider for the catalytic activity of such complexes.

Acknowledgment. This work was funded in part by the Australian Research Council.

IC0345525

(11) Dimitrou, K.; Brown, A. D.; Concolino, T. E.; Rheingold, A. L.; Christou, G. *J. Chem. Soc., Chem. Commun.* **2001**, 1284.

(12) Cotton, F. A.; Lewis, G. E.; Mott, G. N. *Inorg. Chem.* **1982**, *21*, 3127.